JBC RESEARCH ARTICLE

Photoprotective energy quenching in the red alga *Porphyridium purpureum* occurs at the core antenna of the photosystem II but not at its reaction center

Received for publication, December 23, 2021, and in revised form, February 24, 2022 Published, Papers in Press, March 2, 2022,
https://doi.org/10.1016/j.jbc.2022.101783

Yuan Fang[1,2,‡], **Dongyang Liu**[1,2,‡], **Jingjing Jiang**[1], **Axin He**[3], **Rui Zhu**[4], **and Lijin Tian**[1,*]

From the [1]*Key Laboratory of Photobiology, Institute of Botany, Chinese Academy of Sciences, Beijing, China;* [2]*University of Chinese Academy of Sciences, Beijing, China;* [3]*State Key Laboratory for Artificial Microstructures and Mesoscopic Physics, and* [4]*Electron Microscopy Laboratory, School of Physics, Peking University, Beijing, China*

Edited by Joseph Jez

Photosynthetic organisms have evolved light-harvesting antennae over time. In cyanobacteria, external phycobilisomes (PBSs) are the dominant antennae, whereas in green algae and higher plants, PBSs have been replaced by proteins of the Lhc family that are integrated in the membrane. Red algae represent an evolutionary intermediate between these two systems, as they employ both PBSs and membrane LHCR proteins as light-harvesting units. Understanding how red algae cope with light is not only interesting for biotechnological applications, but is also of evolutionary interest. For example, energy-dependent quenching (qE) is an essential photoprotective mechanism widely used by species from cyanobacteria to higher plants to avoid light damage; however, the quenching mechanism in red algae remains largely unexplored. Here, we used both pulse amplitude-modulated (PAM) and time-resolved chlorophyll fluorescence to characterize qE kinetics in the red alga *Porphyridium purpureum*. PAM traces confirmed that qE in *P. purpureum* is activated by a decrease in the thylakoid lumen pH, whereas time-resolved fluorescence results further revealed the quenching site and ultrafast quenching kinetics. We found that quenching exclusively takes place in the photosystem II (PSII) complexes and preferentially occurs at PSII's core antenna rather than at its reaction center, with an overall quenching rate of 17.6 ± 3.0 ns^{-1}. In conclusion, we propose that qE in red algae is not a reaction center type of quenching, and that there might be a membrane-bound protein that resembles PsbS of higher plants or LHCSR of green algae that senses low luminal pH and triggers qE in red algae.

Primary endosymbiotic events gave rise to three branches of photosynthetic eukaryotes: the red algae, the green algae, and the glaucophytes. From these branches, various photosynthetic organisms have evolved adapted to different environments (1). Red algae belong to the most primitive eukaryotic algae (2, 3), which are widespread in both marine and freshwater where they play significant ecological roles (4). Red algae also contain unique polysaccharides, proteins, and other organic substances (5, 6), which have been widely used in food, pharmaceutical products, and in many other fields of industry (7, 8). Because of its distinct evolutionary position and its ecological and commercial importance, the number of studies on red algae is increasing rapidly. However, compared with the green lineages, the understanding of their photosynthetic processes, especially their regulatory mechanisms, lags far behind.

Photosynthetic organisms capture sunlight by using complex light-harvesting antennae that bind a network of pigments to funnel the excitation energy to the reaction centers of photosystem I (PSI) and photosystem II (PSII), where charge separations take place (9, 10). PSI in red algae uses transmembrane proteins of light-harvesting complex I (termed LHCRs) encoded by lhcr genes as antenna (11, 12). These LHCR proteins belong to the LHC superfamily in eukaryotic organism (11, 13). Unlike PSI, the PSII core complex in red algae does not have any additional membrane-intrinsic antenna (14), but uses water-soluble proteins: phycobilisomes, similar to cyanobacteria (15, 16). In the last decade, the structures of PSI-LHCRs and PSII of the red alga *Cyanidioschyzon merolae* have been determined at the atomic level, showing that the core complex moiety from cyanobacteria was largely inherited and additional new subunits typical for eukaryotic oxygenic organisms evolved (17, 18). Clearly, the photosynthetic machinery of red algae has the characteristics of both cyanobacteria and green algae, being endowed with unique light harvesting and energy transfer kinetics.

Photosynthetic organisms have to control the balance between efficient light harvesting at low light intensities and efficient dissipation of excess light energy at high light intensities. This challenge is further complicated by rapid changes in the light intensity occurring during the day on land, but also in tidal habitats in the sea (19). Without regulatory mechanisms that can rapidly respond to increases in the light intensity, the photosynthetic apparatus would suffer severe photodamage (9). This rapid energy dissipation process of green algae and vascular plants is termed energy-dependent quenching (qE). It is one of the nonphotochemical quenching (NPQ) processes (normally the dominant one) that cause a decrease of the maximum fluorescence intensity as reviewed in (9, 20, 21). qE is essential for the optimum growth of plants,

‡ These authors contributed equally to this work.
* For correspondence: Lijin Tian, ltian@ibcas.ac.cn.

and photosynthetic mutants that have an impaired qE capacity have a limited tolerance to high light, which may even lead to the death of these organisms in extreme cases (22). Because of its significant physiological role, it has been intensively investigated in the past decades. Chlorophyll fluorescence-based techniques have been shown to be invaluable probes for energy dissipation processes (23). Photoexcited chlorophyll relaxes to its ground states mainly *via* three pathways: energy transfer to the RC to drive charge separations; the intrinsic radiative decay, namely fluorescence, and nonradiative decay in the form of heat. qE reflects an increase in the rate constant for dissipation of excitation energy as heat. These three pathways compete with each other. Stable charge separations can be blocked by closing the reaction centers (24, 25), which reduces the system to competition between fluorescence and heat dissipation. An increase in the rate constant for heat dissipation (*via* qE) decreases the maximum chlorophyll fluorescence intensity. Thus, chlorophyll fluorescence has been routinely used as a noninvasive probe to study this process either on a timescale of minutes or on an ultrafast timescales from femtoseconds to nanoseconds (26, 27).

In both eukaryotic algae and higher plants, qE is a reversible short-term feedback mechanism regulating the dissipation of excess light energy under high light conditions. In this process the light-harvesting complex stress-related proteins (LHCSR, also called LHCX in diatoms) and photosystem II subunit S (PsbS) are the key regulators for algae and higher plants, respectively (22, 28). Both proteins are sensitive to the lumen pH. Under high light, the thylakoid lumen becomes acidic, thereby inducing protonation of the c-terminus of LHCSR (29) or the helixes of H2 and H3 in PsbS, which triggers conformational changes of light-harvesting proteins to their qE states (30, 31). LHCSRs are pigments-binding proteins, which have the potential to quench the excitation energy (32, 33), while PsbS is pigment free and thus has to interact with other cofactors, such as lutein and zeaxanthin, which can dissipate excitation energy (34–36). Thus far, a similar, specific, photoprotective protein has not yet been identified in red algae (20). In addition, the activation process of qE and the possible quenching sites are still unclear. It has been documented that in *Rhodella violacea* and in *Porphyridium cruentum*, qE is ΔpH-dependent (37), but it is not the case in another type of red alga, *Dixoniella giordanoi*, as recently reported (38). Regarding the quenching site, the LHC antenna system of PSII is one of the quenching targets in green algae and higher plants (33, 39), but so far there is no evidence that LHCs attach to PSII acting as antennae in red algae (14, 40). Therefore, the quenching site may be further narrowed down to either the PSII core antenna or the reaction centers (RC). Currently it is unclear where the quenching sites are localized, and further experimental studies are necessary to clarify this point. Other key questions that already have been addressed in detail in higher plants are, *e.g.*, what are the kinetics of this type of qE and whether PSI is directly quenched, remain to be explored in red algae.

Here, we checked the qE level and its ΔpH-dependence by recording the pulse-amplitude-modulated chlorophyll fluorescence traces of unicellular red algae *Porphyridium purpureum* (also named *P. cruentum*). And we performed spectrally resolved picosecond fluorescence measurements on cells in both unquenched and quenched states. With the use of both global and target analysis, we further identified the PSII core antenna as the quenching site and numerically quantified the ultrafast kinetics of both light harvesting and qE in this type of red algae.

Results

Fluorescence quenching of red algae cells is triggered by ΔpH

The qE capacity of photosynthetic organisms is highly dynamic and depends on the growth conditions (41–44). To check if this species of red algae shows qE, PAM chlorophyll fluorescence of dark-adapted cells was measured. A rapid fluorescence induction was observed upon high light illumination, and the quenching reached a maximum NPQ value around 0.9 within ∼100 s (Fig. 1*A*). In darkness, the quenching level was maintained without noticeable relaxation. However, following the addition of the membrane uncoupler nigericin, it relaxed completely, reaching even higher fluorescence levels than in the dark-adapted state (45). This suggests that this type of quenching is ΔpH-dependent (Fig. 1*A*). With these data, qE formation in the cells under our growing conditions could be successfully quantified. The fact that the fluorescence level on addition of nigericin was higher than that of the dark-acclimated state indicates that there are also other energy regulatory processes involved. Indeed, earlier reports demonstrated that state transitions, another type of short-term regulation, occur in many photosynthetic organisms (46–48). They could co-occur with qE during high light illumination (46, 49). Unfortunately, state transitions have spectral features similar to those of qE, making it hard to separate them (49). In this work, a chemical approach was employed for this purpose. First, cells were locked in state I by following an established protocol (50). DCMU [3-(3,4-dichlorophenyl)-1,1-dimethylurea] and HA (hydroxylamine) were used to block electron transfer from Q_A to Q_B and prevent at the same time recombination between Q_A^- and the PSII donor side. Simultaneously, weak light illumination enabled PSI to drain the electrons from the plastoquinone (PQ) pool. Note that HA has no effect on fluorescence quenching (Fig. S1). Along with the oxidation of the PQ pool, the fluorescence of the cells gradually increased to a stable state I level. Subsequently, acetic acid (HAC) was added to lower the pH and thereby induce fluorescence quenching (Fig. 1*B*). This treatment mimics the luminal pH drop that triggers qE (27, 51). Finally, the fluorescence emission was restored by adjusting the pH to 7.6 by the addition of KOH. This demonstrates that the quenching is largely reversible (Fig. 1*B*). The pH titration curve shows that the fluorescence quenching starts at pH 6.4 and reaches its maximum value at pH 5.0 (Fig. 1*C*). The above results indicate that the use of weak-acid-induced quenching allows us to study the qE process of cells in State I, thus excluding fluorescence changes caused by state transitions.

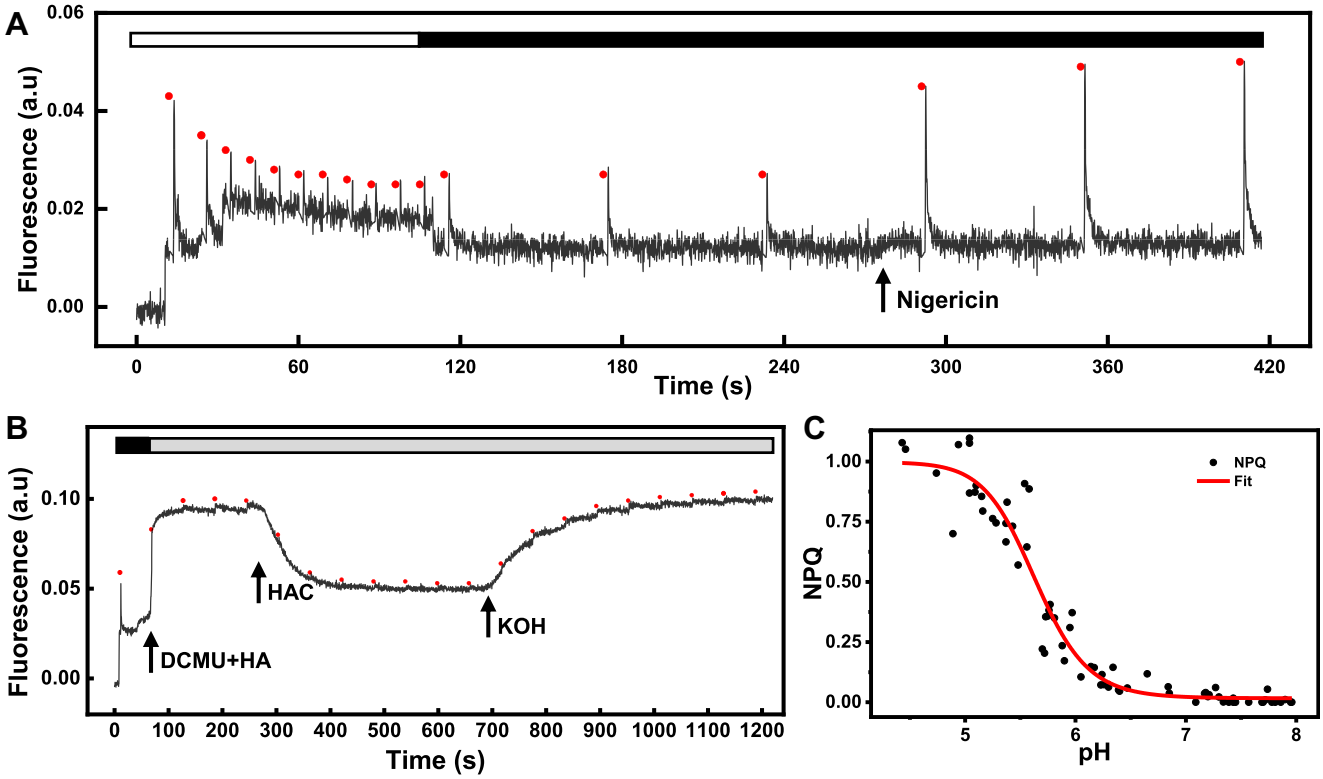

Figure 1. PAM Chl fluorometer traces of *P. purpureum*. The *gray curves* represent Chl fluorescence of cells undergo high light illumination (*white bar*) and dark relaxation (*black bar*), and the *red plots* represent the maximum fluorescence (Fm′) induced by each saturating pulse. *A*, the quenching relaxes following the addition of nigericin (100 μM). *B*, Quenching was also induced at pH 5.5 when acetic acid was added to the cell solution, and the fluorescence intensity was restored when the pH was adjusted back to 7.6 by adding KOH. The NPQ was 0.92 ± 0.14 in P. purpureum cells. Note that, the cells were kept under weak light (25 μmol photons·m^{-2}·s^{-1}, *gray bar*) in the presence of DCMU and HA (100 μM) to state 1. Six biological replicas were measured for all measurements. *C*, pH titration curve in cells. The pH titration curve was obtained by sequentially adding 2 μl acetic acid (1.75 M stock solution) in the presence of nigericin (100 μM). Six biological replicas were measured for cells. The fitted curve is a polynomial function (y = A2 + (A1-A2)/(1 + (x/x0)-p)), yielding x0 (the midpoint pH) of 5.64 ± 0.04. Data are expressed as mean ± SD of six independent experiments.

Quenching occurs in the chlorophylls associated with the photosystems and not in the phycobilisome

The room temperature (RT) absorption spectrum was measured. It contains absorption features typical for both phycobilins (500–670 nm) and Chls (400–500 nm, 630–700 nm) (Fig. S2). To measure the steady-state emission fluorescence of the unquenched (UQ) and quenched (Q) states at RT, excitation at 430 nm and 545 nm was chosen. These wavelengths selectively excite chlorophylls and phycobilisomes, respectively. All the PSII RCs were "closed" by pre-illuminating the cells in the presence of DCMU and HA. We observed a ∼50% fluorescence drop at pH 5.0 (Q) compared with the cells kept at pH 7.5 (UQ). Fluorescence difference spectra ($\Delta F=F_{UQ}-F_Q$) were calculated for each excitation wavelength (Fig. 2, *A* and *B*). Upon 430 nm excitation (Fig. 2*A*), the fluorescence emission peaks at 685 nm and 689 nm for UQ and Q cells, respectively, whereas their difference spectra peak at 683 nm showing a few nanometer blueshift. When the phycobilisomes were excited, the emission spectra showed three peaks, ∼580 nm, 660 nm, and 685 nm, respectively, corresponding to the emission from detached phycoerythrin, the phycobilisomes, and the photosystems. Upon quenching, the emission at 580 nm and 660 nm was hardly affected, whereas the emission at 685 nm was substantially decreased. Taken all these results together, it seems that not the phycobilisomes, but the chlorophylls associated with the photosystems quenched the excitation energy. To confirm the quenching site, time-resolved fluorescence was recorded at three different wavelengths (685 nm, 695 nm, and 720 nm) by using TCSPC (Fig. 2, *C*–*E*). In all cases, Q cells showed a much-accelerated fluorescence decay due to the presence of a quencher. Nonetheless, because the vibration band of PSII fluorescence overlaps with the fluorescence emission of PSI at 700 nm to 800 nm, the TCSPC used here does not have the resolving power to distinguish PSI and PSII fluorescence emission.

The quenching site is PSII rather than PSI

To further investigate the quenching site of qE in *P. purpureum*, time-resolved fluorescence of intact cells with both higher time resolution and spectral resolution was measured with a streak camera system at 77K before and after adding HAC. Low-temperature fluorescence measurements allow a better spectral separation of PSI and PSII, since the former contains "red-chls" that are much more populated at 77K (25). Moreover, to keep the red algae physiologically stable at RT for a long period during the measurement is technically challenging. As directly visible from the streak-camera images,

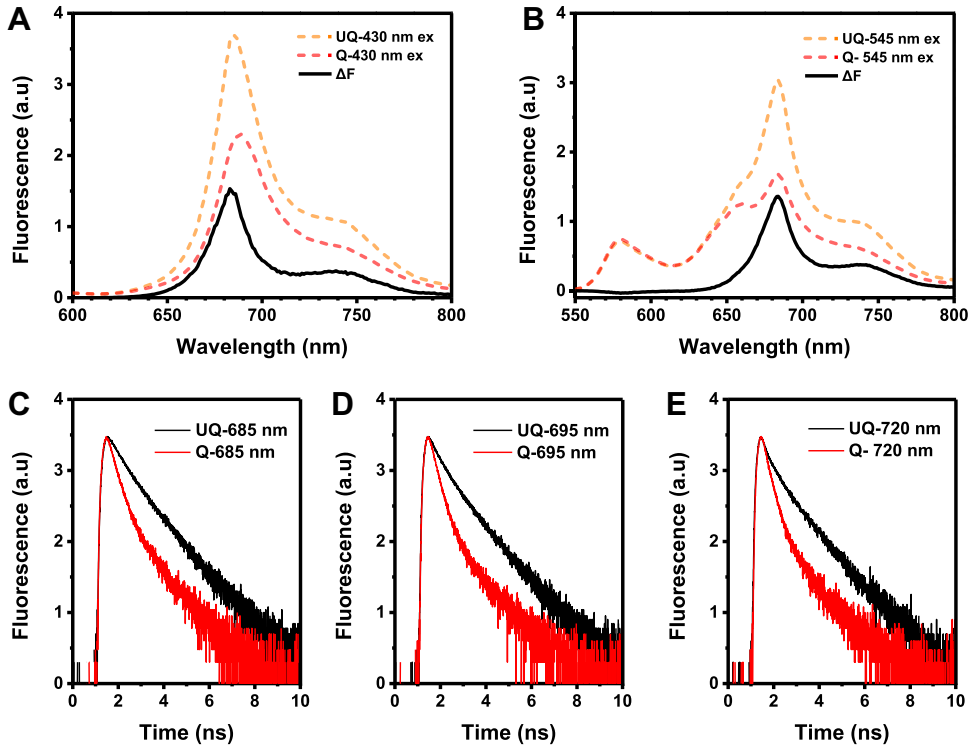

Figure 2. Steady-state spectra and fluorescence lifetime decay curves of *P. purpureum* cells at room temperature. *A* and *B*, fluorescence emission spectra of P. purpureum cells at 430 nm and 545 nm excitation. Both the UQ state (*orange*) and the Q state (*red*) were measured on the same cells at room temperature. The *black line* represents the difference spectrum of UQ versus Q. All spectra were plotted without normalization. *C–E*, the TCSPC fluorescence decay curves of UQ state (*black*) and Q (*red*) state at 685 nm, 695 nm and 720 nm, respectively. The excitation wavelength was 510 nm and the peak counts were equalized for each measurement. Three biological replicas were measured for all measurements.

the fluorescence decay in the PSII region (680–695 nm) was faster at pH 5.5 (Q) compared with 7.0 (UQ) (Fig. 3, A and *B*). This quenching can also be seen in the reconstructed steady-state spectra (Fig. 3*C*) that, together with the fluorescence decay curves at 685 nm and 695 nm, show a clearly faster fluorescence decay (Fig. 3, *D* and *E*). However, in contrast, the fluorescence decay at 720 nm (Fig. 3*F*), largely originating from PSI, was not altered at all by quenching (see other three biological replicates in Fig. S4). These results indicate that the qE quenching in *P. purpureum* predominantly took place in PSII.

Ultrafast kinetics of light harvesting and qE in P. purpureum *at 77K*

To quantitatively describe the kinetics of light harvesting and qE, both global analysis and target analysis were performed. The former provides a pure mathematical description of the data, showing the possible excitation energy transfer processes and the depopulation of low energy states, whereas the latter uses a realistic compartmental model composed of subunits of the photosystems to model (fit) how energy flows from one pool to another. The global analysis required four decay components to obtain a satisfactory fit of the data. The resulting decay-associated spectra (DAS) are shown in Figure 4*A*. The first DAS of 10 ps (black) mainly represents excitation energy transfer from higher energy Chl *a* to lower energy Chl *a*. The second DAS of 112 ps (red) is largely positive, but it has a dip in the red part of the spectrum (~730 nm), which may represent a trapping process in PSII (660–700 nm) and a relatively slow energy transfer process within PSI (700–780 nm). The third DAS of 452 ps represents the slow trapping process in both PSII and PSI. The slowest component has a long lifetime of 2 ns and peaks at 695 nm and 720 nm. This component is a mixture of the decaying of "red-chls" in both PSII and PSI, in agreement with many previous reports (25, 52–54). Regarding the quenching dynamics, the amplitudes of blue and green DAS in the Q state were significantly reduced, by approximately 50%, in the region between 680 nm and 700 nm (Fig. 4, *B* and *C*), whereas the red part between 700 nm and 760 nm was not changed. This indicates that the fluorescence quenching site was in PSII and that it occurred at an earlier stage in energy flow. Otherwise, it would influence the two slowest components very differently.

The PSII core complexes were heavily quenched during qE

The data of UQ and Q cells upon 400 nm excitation were fitted simultaneously to generate the quenching model (Fig. 5*A*). In total, seven compartments were resolved, four of them belonging to PSI, whereas three represent PSII. For the Q state, the PSII part was duplicated in the scheme for clarity (Fig. 5*A*). Estimated from the initial excitation, PSI absorbs roughly 80% of the energy, and the rest was mainly absorbed by PSII, in line with the fact that these cells, like cyanobacteria, contain more PSI than PSII (55). Excitation energy absorbed by the PSI bulk (690 nm) was sequentially transferred to the other three compartments with fluorescence emission peaks at 702 nm, 710 nm, and 715 nm. These results are consistent

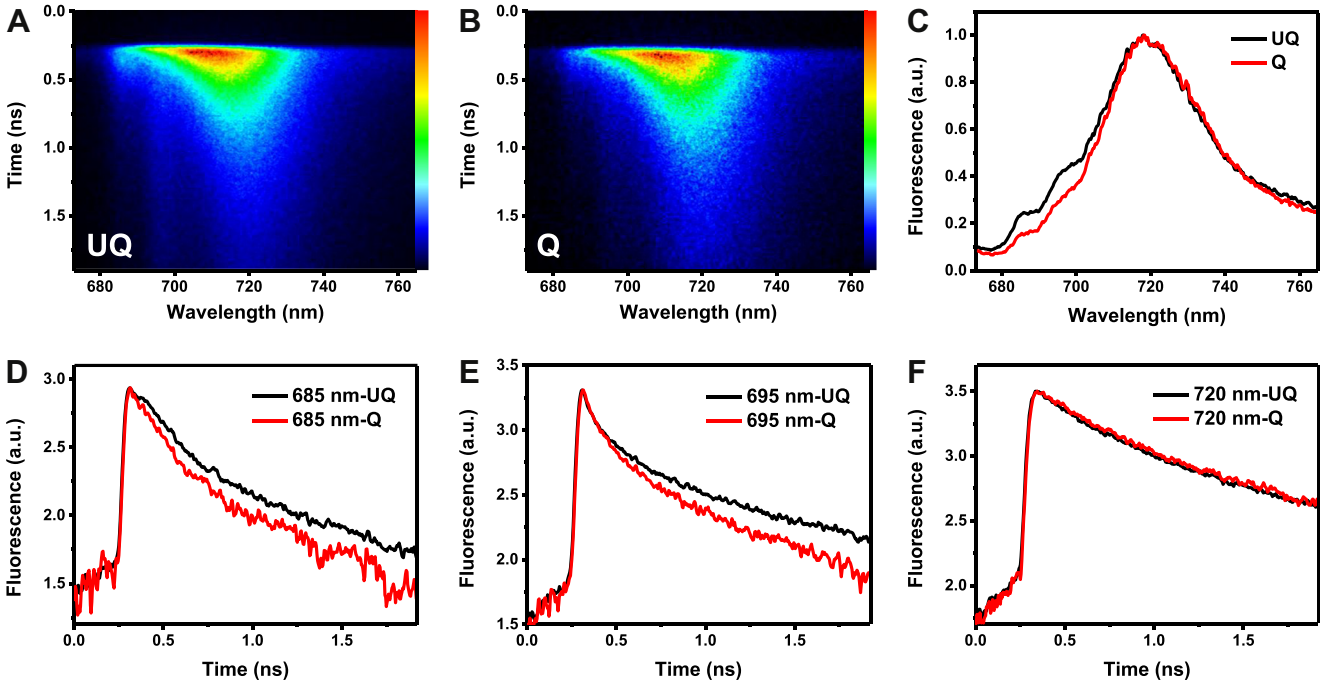

Figure 3. Time-resolved fluorescence data at 77K using 400-nm excitation. *A*, streak-camera images of *P. purpureum* cells in unquenched (UQ) state. *B*, streak-camera images of Porphyridium cells in quenched (Q) state. These images represent the fluorescence intensity (color gradient) as a function of time (vertical axis) and wavelength (horizontal axis); every vertical line represents a fluorescence-decay trace at the corresponding wavelength, while every horizontal line reflects a fluorescence emission spectrum at a certain delay time point. *C*, the reconstructed steady-state spectra of cells in the UQ (*black line*) and Q (*red line*) states. For comparison, they were normalized to their maximum. *D–F*, fluorescence decay curves of cells in UQ state (*black line*) and Q (*red line*) state at 685 nm, 695 nm, and 720 nm. Each pair is normalized to their maximum, respectively. The fluorescence intensity is plotted on a logarithmic time scale.

with the four DAS components of PSI fitted in our global analysis and are largely in agreement with previous reports on PSI kinetics at 77K (25, 27). For PSII, three compartments were resolved, of which two emit at 685 nm. These were set to have an identical spectrum during the fitting. One of the pigment pools emitting at 685 nm carries the initial excitation energy, and it was tentatively assigned to bulk Chls in PSII core complexes, including the higher energy pigments in both CP43 and CP47 subunits. The other compartment emitting at 685 nm possibly originates from the red pigment in CP43. The third compartment, emitting at 695 nm, has a spectrum that is distinct from the others. This compartment probably reflects the red forms of Chls in CP47. This model is a simplified version of the model proposed in (56). Compared with that model, we left out the radical pairs (RPs), as our datasets have a limited resolving power with respect to these nonfluorescent compartments. Nevertheless, the model can distinguish between different interpretations and remains informative. For several other models that were tested, either the fitting went completely wrong or the fitting quality dropped sharply.

To determine which compartments of PSII were initially quenched, we allowed an additional quenching pathway for

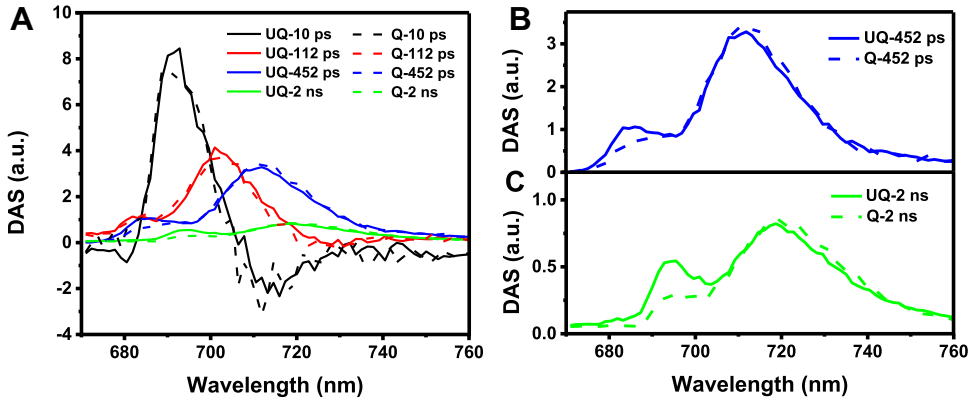

Figure 4. Decay-associated spectra (DAS) of UQ and Q at 77K in *P. purpureum*. *A*, DAS of cells in both UQ (*solid lines*) and Q (*dashed lines*) states, they are normalized to emission spectra at time 0. The corresponding lifetimes are indicated in the figure, note that, for comparison reason, lifetimes were forced to be the same during the fitting for UQ and Q states. *B* and *C*, DAS of the lifetime component of 400 ps (*blue*) and 2 ns (*green*) plotted in *A* were highlighted again without additional normalization.

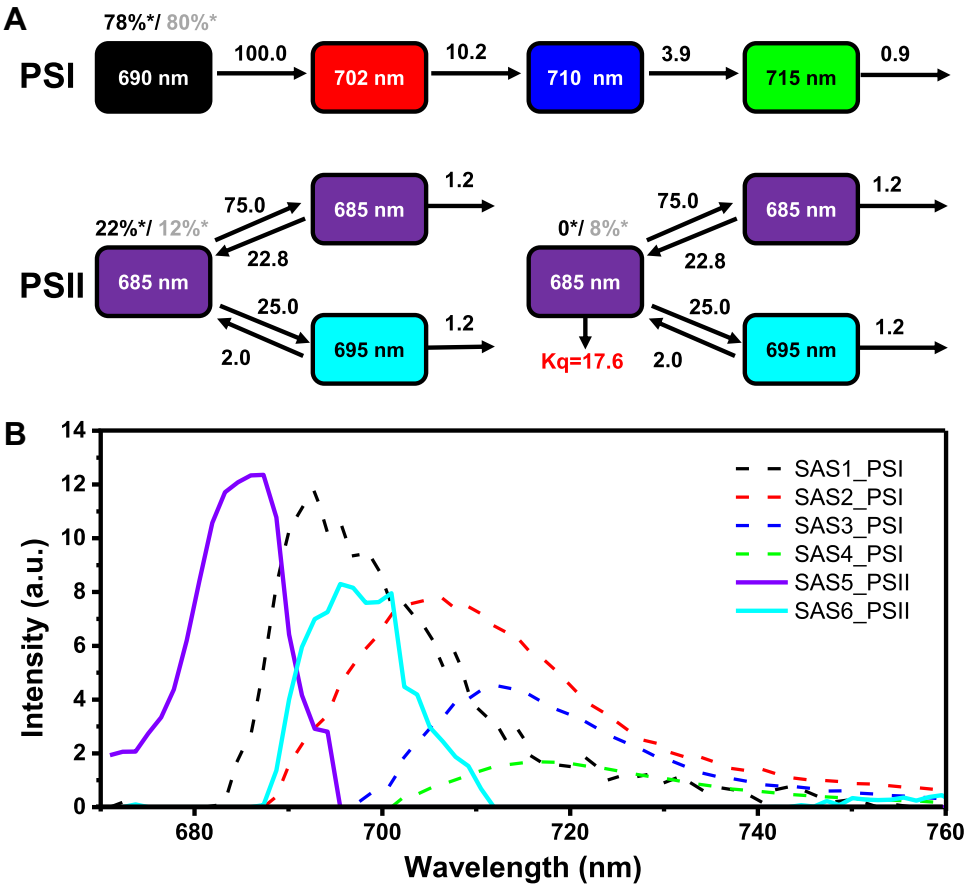

Figure 5. Target analysis results. *A*, schematic model used to describe the time-resolved fluorescence data; Forward and backward energy transfer rates are given in $(ns)^{-1}$, Kq is the quenching rate, and *asterisks* indicate the initial excitations at 400 nm of UQ (*black*) and Q (*gray*). *B*, species-associated spectra (SASs) of each compartment. PSII related SASs, each spectrum was plotted in the same color as its corresponding compartment in *A*.

each pool in turn, and we found that the most satisfactory fitting could only be obtained when the bulk Chls were set to quench. Moreover, we noticed that not all the PSII was quenched under our conditions, but only 40–50% of them (varying slightly among replicates). Finally, the quenching rate was estimated to be 17.6 ± 3.0 ns^{-1}.

Discussion

qE in P. purpureum *is ΔpH-dependent*

While it has been well documented that in green algae, mosses, and higher plants, the qE process is activated by low luminal pH, it remains controversial in red algae (37, 38). Delphin *et al.* found that in the presence of the membrane uncouplers NH_4Cl or nigericin, the fluorescence of the *R. violacea* and *P. purpureum* cells is no longer quenched by high light (37). However, Fattore *et al.* (38) later found that nigericin-treated *D. giordanoi* cells still performed quenching in response to high light, and their NPQ rose with the increase of the actinic light intensity. Note that in their experiments, the far-red light was turned off during the measurements, which should be kept on to keep the cells in state I. Here, we performed the same experiment again using *P. purpureum* and found that the qE process is indeed activated by a low lumen pH, in line with previous results (37, 46, 57). We speculate that in the study of *D. giordanoi*, State II may have been induced under high light illumination, even in the presence of nigericin, which then led to qE-like fluorescence quenching. Nevertheless, biodiversity in qE mechanisms among different species within the Class of Rhodophyceae should not be excluded.

Phycobilisome and PSI are not quenched

Here, we provided direct evidence to show that qE in red algae takes place predominantly in the PSII complexes. In principal, all pigment-binding photosynthetic subunits including PSII core complex, PSI core complex, and their peripheral antenna LHCs could potentially be the initial target of quenching, and indeed in the green lineage, it was found that the quenching site is nonspecific (33, 35, 39, 58–60). In contrast, in cyanobacteria, the qE occurs specifically in phycobilisomes, and the orange carotenoid protein (OCP) is indispensable for this process. Red algae also contain phycobilisomes; however, the gene encoding OCP protein is lacking (61). This rules out this phycobilisome-OCP type of quenching. This is consistent with our observation that the emission at 660 nm from phycobilisomes was not changed upon quenching. Another question is if other photosynthetic complexes, such as PSII core, PSI (PSI core plus its antenna

LHCRs), are quenched. Our ultrafast fluorescence spectroscopic results precisely separated the kinetics of PSI and PSII. These measurements clearly demonstrated that only PSII was affected by qE, at least in cells that were kept in state I.

The quenching does not occur in the RC

PSII core complex is further composed of the reaction center (RC) and two core antenna proteins, CP43 and CP47. Kirilovsky and colleagues (37) suggested that the PSII fluorescence quenching might occur in the reaction center other than its core antenna because the minimal fluorescence was not quenched during qE. A similar opinion was expressed by Krupnik *et al.* (57). They observed a reaction center-based quencher in red algae by measuring isolated PSII complexes at low pH. However, our data favor the view that qE occurs in the antenna and not in the RC itself. In the first place, we would like to emphasize that using F_0 quenching as an indicator for the presence of an RC-based quencher should be reconsidered. An interesting study on *Arabidopsis* has pointed out that qE might function differently in RCs that are in the open and closed state, respectively (62), making F_0 a less reliable indicator. Moreover, the F_0 after high light illumination might not represent the true F_0 anymore, since the PQ pool is likely to remain partially reduced considering the additional electron feed-in *via* NADPH dehydrogenase in darkness (nonphotochemical reduction of the PQ pool). Secondly, in an RC-based quenching model, the quencher was assigned to the Chl cation $P680^+$ (57, 63), a radical formed during charge separation, but in our case cells were kept in complete darkness, and addition of a weak acid won't create excitons. One may doubt if weak-acid-induced quenching equates the biological process of qE. Regarding this question, in a previous study we have established a solid correlation between weak-acid-induced quenching and the expression of LHCSR proteins in the *Chlamydomonas* system (27). It was, however, not practical to use this approach for red algae since no qE-defective mutant of red algae was available. Nevertheless, the chance that these two quenching processes, light-induced and weak-acid-induced, are different is very small in our opinion.

The quencher is highly effective but unknown

The quenching rate was estimated to be 17.6 ± 3.0 ns^{-1}, which corresponds to a lifetime of 55 ps, PSII core complexes contain 35 chlorophylls, if we count one quencher per dimer, that would mean under the scheme of ultrafast equilibrium, the slowest quenching time per Chl is about 55 ps/70 = 0.78 ps, which is extremely fast. On the other hand, this fast quenching rate is not surprising, several reported rates on the single molecule level in different quenching systems are even faster (27, 64, 65). It seems that this high rate of quenching is essential for the qE process to outcompete photochemical quenching, which is equally fast (subpicosecond). And only in this way it could guarantee an effective photoprotection, even for open RCs. One question that arises here is: what exactly is the nature of this ultrafast quencher? Photoprotective proteins such as PsbS, LHCSR, and LHCX are the key players of qE in vascular plants, green algae, moss, and diatoms, respectively (20, 66). Given the fact that qE in red algae can also be triggered by a low luminal pH and that it belongs to an antenna type of quenching, we suggest that there may be a membrane-bound protein that resembles PsbS in higher plants or LHCX/SR in branches of green algae and mosses being responsible for the observed energy dissipation in PSII.

Experimental procedures

Algae culture

P. purpureum strain FACHB-840 was purchased from the Freshwater Algae Culture Collection at the Institute of Hydrobiology (FACHB). Cells were cultured in artificial sea water (ASW) medium (Andersen *et al.* 2005) at 25 °C under continuous white light (25 μmol photons·m^{-2}·s^{-1}). The liquid culture was kept on a shaker at 100 rpm.

PAM fluorescence measurement

The chlorophyll fluorescence curve in Figures. 1 and 2 was measured with a pulse amplitude modulation fluorometer (Dual-PAM-100; Heinz Walz GmbH). Saturating light (6000 μmol photons·m^{-2}·s^{-1}, 250 ms) and actinic light (1500 μmol photons·m^{-2}·s^{-1}) were used; NPQ was calculated as NPQ=(F_m-$F_{m'}$)/$F_{m'}$. All cells were dark adapted for at least 15 min before measurements.

Acetic-acid-induced chlorophyll fluorescence quenching

Before measurements, the cells were washed and resuspended with fresh ASW medium (pH 7.6). To keep the cells in State 1, they were preilluminated under low light (25 μmol photons·m^{-2}·s^{-1}) in the presence of 100 μM DCMU and 1 mM HA. Acetic acid (1.75 M stock solution) was used to tune the pH down to 5.0, and KOH (1.75 M) was used to adjust the pH back to 7.6. In Figure. 1*B*, 100 μM nigericin was added to dissipate the pH difference over the thylakoid membrane.

Steady-state fluorescence spectroscopy

Fluorescence emission spectra were recorded on an FLS1000 Photoluminescence Spectrometer (Edinburgh). Cells were resuspended in artificial sea water and directly measured in a 10*10*40 mm quartz cuvette at room temperature. The sample OD at the maximum emission in the red region of the spectrum was adjusted between 0.1 and 0.15 for fluorescence measurements. Magnetic stirring was on to prevent cell sedimentation. In all measurements, a bandwidth of 3 nm was used for both excitation and emission, and the step size was 1 nm. An optical long-pass filter (550) nm was placed before the detector to remove scattered light.

Time-resolved fluorescence

Fluorescence lifetime decay measurements of *P. purpureum* cells at room temperature were performed with a time-correlated single photon counting setup (Edinburgh FLS1000). A picosecond diode laser (EPL Series,510 nm) with a repetition rate of 10 MHz was used for excitation. Sample

OD at 670 nm was adjusted between 0.1 and 0.15 to avoid significant self-absorption. For measuring cells during quenching, cells were kept in a fully quenched state by adding acetic acid as aforementioned, and to ensure the PSII RCs were in a homogeneous closed state, 100 μM DCMU and 1 mM HA were added for both the UQ and Q states.

Time-resolved fluorescence at 77K was recorded with a subpicosecond streak-camera system (HAMAMATSU Universal Streak camera C10910) combined with a spectrograph (Princeton Instruments Acton SpectraPro SP-2300, grating of 150 grooves/mm, blaze wavelength 500 nm). A CW DPSS green laser (Spectra-Physics Millennia eV) pumped a Ti:Sapphire ultrafast oscillator (Spectra-Physics Tsunami Series). This laser was used to produce ultrashort pulses at 800 nm (repetition rate of 80 MHz), and its second harmonic (400 nm) was used for excitation. Power-dependent studies showed that the observed decays were annihilation-free, see Fig. S3. The samples were kept in liquid nitrogen in a cold finger, and their optical density at 670 nm was ∼1.0 with 3 mm optical path. Scattered light was removed with a long-pass optical filter (550 nm). For each fluorescence measurement, a high signal/noise ratio was achieved by averaging a sequence of 150 single images with a CCD exposure time of 10 s for each image.

Global and target analysis

Data obtained with the streak-camera setup were globally analyzed with the R package TIMP-based Glotaran, and for details of the methodology of global and target analysis, see refs. (67, 68). In our data, the typical FWHM value of the instrument response function IRF (t, λ) was estimated to be 12 ps. For global analysis, singular value decomposition results suggest that a minimum model of four decay components was necessary to satisfactorily fit the data. For direct comparison, all four lifetimes were linked (forced to be identical) between UQ and Q states.

Target analysis would allow us to directly reveal the quenching site and rate. Here, seven compartments were resolved in our target analysis. A set of constraints were used: (1) nonnegative least squares were applied; (2) the two compartments of 685 nm in purple were set to have an identical spectrum during the fitting; (3) the initial excitations were fixed during the fitting; (4) zero constraints were used on photosystem I compartments: amplitudes of the SAS were forced to be zero, up to 680 nm (black), 685 nm (red), 695 nm (blue), and 700 nm (green), respectively.

Both global and target analyses were performed on four biological replicas using a same set parameter, and the results were largely reproducible (Fig. S5).

Data availability

All data described are contained within the article.

Supporting information—This article contains supporting information.

Acknowledgments—We thank Dr Gert Schansker for useful discussions. This work is supported by grants from the National Key Research and Development Program of China (Grant No. 2019YFA0904604), the National Natural Science Foundation of China (Grant Nos.11804172, 31970381, 11605001, 91850104).

Author contributions—Y. F., D. L., and L. T. formal analysis; Y. F., D. L., J. J., A. H., R. Z., and L. T. investigation; L. T. methodology; Y. F., D. L., and L. T. writing—original draft.

Conflict of interest—The authors declare that they have no conflicts of interest with the contents of this article.

Abbreviations—The abbreviations used are: ASW, artificial sea water; DCMU, 3-(3,4-dichlorophenyl)-1,1-dimethylurea; DAS, decay-associated spectra; HA, hydroxylamine; LHC, light-harvesting complex; LHCSR, light-harvesting complex stress-related proteins; NPQ, non-photochemcial quenching; OCP, orange carotenoid protein; PMSF, phenylmethylsulfonyl fluoride; PSI, photosystem I; PSII, photosystem II; PsbS, photosystem II subunit S; PQ, plastoquinol; PAM, pulse-amplitude-modulated; Q, quenched state; qE, energy-dependent quenching; RPs, radical pairs; RC, reaction center; RT, room temperature; SAS, Species-associated spectra; qT, state transitions; UQ, unquenched state.

References

1. Bhattacharya, D., Yoon, H. S., and Hackett, J. D. (2004) Photosynthetic eukaryotes unite: Endosymbiosis connects the dots. *Bioessays* **26**, 50–60
2. Keeling, P. J. (2013) The number, speed, and impact of plastid endosymbioses in eukaryotic evolution. *Annu. Rev. Plant Biol.* **64**, 583–607
3. Stiller, J. W., and Hall, B. D. (1997) The origin of red algae: Implications for plastid evolution. *Proc. Natl. Acad. Sci. U. S. A.* **94**, 4520–4525
4. Guiry, M. D. (2012) How many species of algae are there? *J. Phycol.* **48**, 1057–1063
5. Yu, P., Wu, Y., Wang, G., Jia, T., and Zhang, Y. (2017) Purification and bioactivities of phycocyanin. *Crit. Rev. Food Sci. Nutr.* **57**, 3840–3849
6. Cian, R. E., Drago, S. R., de Medina, F. S., and Martinez-Augustin, O. (2015) Proteins and carbohydrates from red seaweeds: Evidence for beneficial effects on gut function and microbiota. *Mar. Drugs* **13**, 5358–5383
7. Usov, A. I. (2011) Polysaccharides of the red algae. *Adv. Carbohydr. Chem. Biochem.* **65**, 115–217
8. Wang, H. D., Chen, C. C., Huynh, P., and Chang, J. S. (2015) Exploring the potential of using algae in cosmetics. *Bioresour. Technol.* **184**, 355–362
9. Rochaix, J. D. (2014) Regulation and dynamics of the light-harvesting system. *Annu. Rev. Plant Biol.* **65**, 287–309
10. Croce, R., and van Amerongen, H. (2020) Light harvesting in oxygenic photosynthesis: Structural biology meets spectroscopy. *Science* **369**, eaay2058
11. Wolfe, G. R., Cunningham, F. X., Durnford, D., Green, B. R., and Gantt, E. (1994) Evidence for a common origin of chloroplasts with light-harvesting complexes of different pigmentation. *Nature* **367**, 566–568
12. Busch, A., Nield, J., and Hippler, M. (2010) The composition and structure of photosystem I-associated antenna from *Cyanidioschyzon merolae*. *Plant J.* **62**, 886–897
13. Neilson, J. A., and Durnford, D. G. (2010) Structural and functional diversification of the light-harvesting complexes in photosynthetic eukaryotes. *Photosynth. Res.* **106**, 57–71
14. Gardian, Z., Bumba, L., Schrofel, A., Herbstova, M., Nebesarova, J., and Vacha, F. (2007) Organisation of photosystem I and photosystem II in red alga *Cyanidium caldarium*: Encounter of cyanobacterial and higher plant concepts. *Biochim. Biophys. Acta* **1767**, 725–731
15. Calzadilla, P. I., and Kirilovsky, D. (2020) Revisiting cyanobacterial state transitions. *Photochem. Photobiol. Sci.* **19**, 585–603
16. Ho, M. Y., Soulier, N. T., Canniffe, D. P., Shen, G., and Bryant, D. A. (2017) Light regulation of pigment and photosystem biosynthesis in cyanobacteria. *Curr. Opin. Plant Biol.* **37**, 24–33

17. Ago, H., Adachi, H., Umena, Y., Tashiro, T., Kawakami, K., Kamiya, N., Tian, L., Han, G., Kuang, T., Liu, Z., Wang, F., Zou, H., Enami, I., Miyano, M., and Shen, J. R. (2016) Novel features of eukaryotic photosystem II revealed by its crystal structure analysis from a red alga. *J. Biol. Chem.* **291**, 5676–5687
18. Pi, X., Tian, L., Dai, H. E., Qin, X., Cheng, L., Kuang, T., Sui, S. F., and Shen, J. R. (2018) Unique organization of photosystem I-light-harvesting supercomplex revealed by cryo-EM from a red alga. *Proc. Natl. Acad. Sci. U. S. A.* **115**, 4423–4428
19. Croce, R., and van Amerongen, H. (2014) Natural strategies for photosynthetic light harvesting. *Nat. Chem. Biol.* **10**, 492–501
20. Niyogi, K. K., and Truong, T. B. (2013) Evolution of flexible non-photochemical quenching mechanisms that regulate light harvesting in oxygenic photosynthesis. *Curr. Opin. Plant Biol.* **16**, 307–314
21. Murchie, E. H., and Ruban, A. V. (2020) Dynamic non-photochemical quenching in plants: From molecular mechanism to productivity. *Plant J.* **101**, 885–896
22. Peers, G., Truong, T. B., Ostendorf, E., Busch, A., Elrad, D., Grossman, A. R., Hippler, M., and Niyogi, K. K. (2009) An ancient light-harvesting protein is critical for the regulation of algal photosynthesis. *Nature* **462**, 518–521
23. Kalaji, H. M., Schansker, G., Ladle, R. J., Goltsev, V., Bosa, K., Allakhverdiev, S. I., Brestic, M., Bussotti, F., Calatayud, A., Dabrowski, P., Elsheery, N. I., Ferroni, L., Guidi, L., Hogewoning, S. W., Jajoo, A., *et al.* (2014) Frequently asked questions about *in vivo* chlorophyll fluorescence: Practical issues. *Photosynth. Res.* **122**, 121–158
24. Wientjes, E., and Croce, R. (2012) Pms: photosystem I electron donor or fluorescence quencher. *Photosynth. Res.* **111**, 185–191
25. Tian, L., Farooq, S., and van Amerongen, H. (2013) Probing the picosecond kinetics of the photosystem II core complex *in vivo*. *Phys. Chem. Chem. Phys.* **15**, 3146–3154
26. Muller, P., Li, X. P., and Niyogi, K. K. (2001) Non-photochemical quenching. A response to excess light energy. *Plant Physiol.* **125**, 1558–1566
27. Tian, L., Nawrocki, W. J., Liu, X., Polukhina, I., van Stokkum, I. H. M., and Croce, R. (2019) pH dependence, kinetics and light-harvesting regulation of nonphotochemical quenching in *Chlamydomonas*. *Proc. Natl. Acad. Sci. U. S. A.* **116**, 8320–8325
28. Li, X. P., Bjorkman, O., Shih, C., Grossman, A. R., Rosenquist, M., Jansson, S., and Niyogi, K. K. (2000) A pigment-binding protein essential for regulation of photosynthetic light harvesting. *Nature* **403**, 391–395
29. Liguori, N., Roy, L. M., Opacic, M., Durand, G., and Croce, R. (2013) Regulation of light harvesting in the green alga *Chlamydomonas reinhardtii*: The C-terminus of LHCSR is the knob of a dimmer switch. *J. Am. Chem. Soc.* **135**, 18339–18342
30. Krishnan-Schmieden, M., Konold, P. E., Kennis, J. T. M., and Pandit, A. (2021) The molecular pH-response mechanism of the plant light-stress sensor PsbS. *Nat. Commun.* **12**, 2291
31. Liguori, N., Campos, S. R. R., Baptista, A. M., and Croce, R. (2019) Molecular anatomy of plant photoprotective switches: The sensitivity of PsbS to the environment, residue by residue. *J. Phys. Chem. Lett.* **10**, 1737–1742
32. Bonente, G., Ballottari, M., Truong, T. B., Morosinotto, T., Ahn, T. K., Fleming, G. R., Niyogi, K. K., and Bassi, R. (2011) Analysis of LhcSR3, a protein essential for feedback de-excitation in the green alga *Chlamydomonas reinhardtii*. *PLoS Biol.* **9**, e1000577
33. Girolomoni, L., Cazzaniga, S., Pinnola, A., Perozeni, F., Ballottari, M., and Bassi, R. (2019) LHCSR3 is a nonphotochemical quencher of both photosystems in *Chlamydomonas reinhardtii*. *Proc. Natl. Acad. Sci. U. S. A.* **116**, 4212–4217
34. Fan, M., Li, M., Liu, Z., Cao, P., Pan, X., Zhang, H., Zhao, X., Zhang, J., and Chang, W. (2015) Crystal structures of the PsbS protein essential for photoprotection in plants. *Nat. Struct. Mol. Biol.* **22**, 729–735
35. Xu, P., Tian, L., Kloz, M., and Croce, R. (2015) Molecular insights into Zeaxanthin-dependent quenching in higher plants. *Sci. Rep.* **5**, 13679
36. Sacharz, J., Giovagnetti, V., Ungerer, P., Mastroianni, G., and Ruban, A. V. (2017) The xanthophyll cycle affects reversible interactions between PsbS and light-harvesting complex II to control non-photochemical quenching. *Nat. Plants* **3**, 16225
37. Delphin, E., Duval, J. C., Etienne, A. L., and Kirilovsky, D. (1998) DeltapH-dependent photosystem II fluorescence quenching induced by saturating, multiturnover pulses in red algae. *Plant Physiol.* **118**, 103–113
38. Fattore, N., Savio, S., Vera-Vives, A. M., Battistuzzi, M., Moro, I., La Rocca, N., and Morosinotto, T. (2021) Acclimation of photosynthetic apparatus in the mesophilic red alga *Dixoniella giordanoi*. *Physiol. Plant* **173**, 805–817
39. Nicol, L., Nawrocki, W. J., and Croce, R. (2019) Disentangling the sites of non-photochemical quenching in vascular plants. *Nat. Plants* **5**, 1177–1183
40. Su, H. N., Xie, B. B., Zhang, X. Y., Zhou, B. C., and Zhang, Y. Z. (2010) The supramolecular architecture, function, and regulation of thylakoid membranes in red algae: An overview. *Photosynth. Res.* **106**, 73–87
41. Gabilly, S. T., Baker, C. R., Wakao, S., Crisanto, T., Guan, K., Bi, K., Guiet, E., Guadagno, C. R., and Niyogi, K. K. (2019) Regulation of photoprotection gene expression in Chlamydomonas by a putative E3 ubiquitin ligase complex and a homolog of CONSTANS. *Proc. Natl. Acad. Sci. U. S. A.* **116**, 17556–17562
42. Allorent, G., Lefebvre-Legendre, L., Chappuis, R., Kuntz, M., Truong, T. B., Niyogi, K. K., Ulm, R., and Goldschmidt-Clermont, M. (2016) UV-B photoreceptor-mediated protection of the photosynthetic machinery in *Chlamydomonas reinhardtii*. *Proc. Natl. Acad. Sci. U. S. A.* **113**, 14864–14869
43. Hong, S. H., Kim, H. J., Ryu, J. S., Choi, H., Jeong, S., Shin, J., Choi, G., and Nam, H. G. (2008) CRY1 inhibits COP1-mediated degradation of BIT1, a MYB transcription factor, to activate blue light-dependent gene expression in *Arabidopsis*. *Plant J.* **55**, 361–371
44. Zhan, J., Steglich, C., Scholz, I., Hess, W. R., and Kirilovsky, D. (2021) Inverse regulation of light harvesting and photoprotection is mediated by a 3'-end-derived sRNA in cyanobacteria. *Plant Cell* **33**, 358–380
45. Finazzi, G., Johnson, G. N., Dall'Osto, L., Zito, F., Bonente, G., Bassi, R., and Wollman, F. A. (2006) Nonphotochemical quenching of chlorophyll fluorescence in *Chlamydomonas reinhardtii*. *Biochemistry* **45**, 1490–1498
46. Delphin, E., Duval, J. C., Etienne, A. L., and Kirilovsky, D. (1996) State transitions or delta pH-dependent quenching of photosystem II fluorescence in red algae. *Biochemistry* **35**, 9435–9445
47. Wesselhoeft, R. A., Kowalski, P. S., and Anderson, D. G. (2018) Engineering circular RNA for potent and stable translation in eukaryotic cells. *Nat. Commun.* **9**, 2629
48. Murata, N. (2009) The discovery of state transitions in photosynthesis 40 years ago. *Photosynth. Res.* **99**, 155–160
49. Allorent, G., Tokutsu, R., Roach, T., Peers, G., Cardol, P., Girard-Bascou, J., Seigneurin-Berny, D., Petroutsos, D., Kuntz, M., Breyton, C., Franck, F., Wollman, F. A., Niyogi, K. K., Krieger-Liszkay, A., Minagawa, J., *et al.* (2013) A dual strategy to cope with high light in *Chlamydomonas reinhardtii*. *Plant Cell* **25**, 545–557
50. Cardol, P., Alric, J., Girard-Bascou, J., Franck, F., Wollman, F. A., and Finazzi, G. (2009) Impaired respiration discloses the physiological significance of state transitions in *Chlamydomonas*. *Proc. Natl. Acad. Sci. U. S. A.* **106**, 15979–15984
51. Endo, T., and Asada, K. (1996) Dark induction of the non-photochemical quenching of chlorophyll fluorescence by acetate in *Chlamydomonas reinhardtii*. *Plant Cell Physiol.* **37**, 551–555
52. Snellenburg, J. J., Wlodarczyk, L. M., Dekker, J. P., van Grondelle, R., and van Stokkum, I. H. (2017) A model for the 77K excited state dynamics in *Chlamydomonas reinhardtii* in state 1 and state 2. *Biochim. Biophys. Acta Bioenerg.* **1858**, 64–72
53. Snellenburg, J. J., Dekker, J. P., van Grondelle, R., and van Stokkum, I. H. (2013) Functional compartmental modeling of the photosystems in the thylakoid membrane at 77 K. *J. Phys. Chem. B* **117**, 11363–11371
54. Ueno, Y., Aikawa, S., Kondo, A., and Akimoto, S. (2015) Light adaptation of the unicellular red alga, Cyanidioschyzon merolae, probed by time-resolved fluorescence spectroscopy. *Photosynth. Res.* **125**, 211–218
55. Luimstra, V. M., Schuurmans, J. M., de Carvalho, C. F. M., Matthijs, H. C. P., Hellingwerf, K. J., and Huisman, J. (2019) Exploring the low photosynthetic efficiency of cyanobacteria in blue light using a mutant lacking phycobilisomes. *Photosynth. Res.* **141**, 291–301

56. Szczepaniak, M., Sander, J., Nowaczyk, M., Muller, M. G., Rogner, M., and Holzwarth, A. R. (2009) Charge separation, stabilization, and protein relaxation in photosystem II core particles with closed reaction center. *Biophys. J.* **96**, 621–631
57. Krupnik, T., Kotabova, E., van Bezouwen, L. S., Mazur, R., Garstka, M., Nixon, P. J., Barber, J., Kana, R., Boekema, E. J., and Kargul, J. (2013) A reaction center-dependent photoprotection mechanism in a highly robust photosystem II from an extremophilic red alga, *Cyanidioschyzon merolae*. *J. Biol. Chem.* **288**, 23529–23542
58. Johnson, M. P., Goral, T. K., Duffy, C. D., Brain, A. P., Mullineaux, C. W., and Ruban, A. V. (2011) Photoprotective energy dissipation involves the reorganization of photosystem II light-harvesting complexes in the grana membranes of spinach chloroplasts. *Plant Cell* **23**, 1468–1479
59. Dall'Osto, L., Cazzaniga, S., Bressan, M., Palecek, D., Zidek, K., Niyogi, K. K., Fleming, G. R., Zigmantas, D., and Bassi, R. (2017) Two mechanisms for dissipation of excess light in monomeric and trimeric light-harvesting complexes. *Nat. Plants* **3**, 17033
60. Pinnola, A., Cazzaniga, S., Alboresi, A., Nevo, R., Levin-Zaidman, S., Reich, Z., and Bassi, R. (2015) Light-harvesting complex stress-related proteins catalyze excess energy dissipation in both photosystems of *Physcomitrella patens*. *Plant Cell* **27**, 3213–3227
61. Bhattacharya, D., Price, D. C., Chan, C. X., Qiu, H., Rose, N., Ball, S., Weber, A. P., Arias, M. C., Henrissat, B., Coutinho, P. M., Krishnan, A., Zauner, S., Morath, S., Hilliou, F., Egizi, A., *et al.* (2013) Genome of the red alga *Porphyridium purpureum*. *Nat. Commun.* **4**, 1941
62. Farooq, S., Chmeliov, J., Wientjes, E., Koehorst, R., Bader, A., Valkunas, L., Trinkunas, G., and van Amerongen, H. (2018) Dynamic feedback of the photosystem II reaction centre on photoprotection in plants. *Nat. Plants* **4**, 225–231
63. Bruce, D., Samson, G., and Carpenter, C. (1997) The origins of non-photochemical quenching of chlorophyll fluorescence in photosynthesis. Direct quenching by P680+ in photosystem II enriched membranes at low pH. *Biochemistry* **36**, 749–755
64. Tian, L., van Stokkum, I. H., Koehorst, R. B., Jongerius, A., Kirilovsky, D., and van Amerongen, H. (2011) Site, rate, and mechanism of photoprotective quenching in cyanobacteria. *J. Am. Chem. Soc.* **133**, 18304–18311
65. Dinc, E., Tian, L., Roy, L. M., Roth, R., Goodenough, U., and Croce, R. (2016) LHCSR1 induces a fast and reversible pH-dependent fluorescence quenching in LHCII in *Chlamydomonas reinhardtii* cells. *Proc. Natl. Acad. Sci. U. S. A.* **113**, 7673–7678
66. Giovagnetti, V., and Ruban, A. V. (2018) The evolution of the photoprotective antenna proteins in oxygenic photosynthetic eukaryotes. *Biochem. Soc. Trans.* **46**, 1263–1277
67. van Stokkum, I. H., Larsen, D. S., and van Grondelle, R. (2004) Global and target analysis of time-resolved spectra. *Biochim. Biophys. Acta* **1657**, 82–104
68. Snellenburg, J. J., Laptenok, S. P., Seger, R., Mullen, K. M., and Stokkum, I. H. M.v. (2012) Glotaran: A java-based graphical user interface for the R package TIMP. *J. Stat. Softw.* **49**, 1–22